

Kinetics of Irreversible Adsorption with Diffusion: Application to Biomolecule Immobilization

D. Brynn Hibbert,* J. Justin Gooding, and Paul Erokhin

School of Chemistry, University of New South Wales, Sydney, NSW 2052, Australia

Received September 6, 2001. In Final Form: November 12, 2001

The kinetics of irreversible adsorption has been modeled numerically for cases for which the rate-limiting process is adsorption through to those for which diffusion to the surface is rate limiting. Comparison with limiting analytical models shows that even for a system under diffusion control the Ilkovic diffusion model with rate proportional to the surface coverage does not describe the kinetics adequately. The best approximate analytical models are a simple first-order model for rate-limiting adsorption and the Ilkovic model for diffusion control. The models were compared to experimental quartz crystal microbalance data for the attachment of glucose oxidase to a self-assembled monolayer. Although none of the limiting analytical models could adequately describe the adsorption behavior of this system, excellent fits to the experimental data were obtained with the numerical model for rate-limiting adsorption with heat of adsorption proportional to coverage (Frumkin adsorption kinetics). Good agreement between the model and published adsorption data was also obtained for antigen adsorption to an antibody-modified surface and for oligonucleotides hybridizing with the surface-bound complementary oligonucleotides.

Introduction

Immobilization of biorecognition molecules and other biomolecules is a key component of many biotechnological applications.^{1,2} As the purpose of immobilization is to maintain the molecule of interest on a solid surface, the biomolecule is usually either covalently attached or strongly adsorbed onto the appropriate surface. During the immobilization process, the biomolecule must diffuse to the surface whereupon it either reacts directly with the binding site or adsorbs nonspecifically to the surface and is thus transported to the binding site via surface diffusion. Once the biomolecule is attached to the binding site, the adsorption process is essentially irreversible. An understanding of the kinetics of this irreversible adsorption is important in ascertaining the appropriate immobilization conditions for the fabrication of the biomolecular surface.

The modern interest in describing the kinetics of adsorption dates to the work of Delahay and co-workers^{3,4} who considered semi-infinite diffusion to plane and spherical electrodes at which adsorption following the Langmuir isotherm occurred. The numerical solutions of Delahay and Fike³ were criticized by Reinmuth⁵ who presented exact and limiting equations, again where adsorption followed the Langmuir isotherm. As both these theories only consider the Langmuir isotherm, the models only apply to biomolecule adsorption where every adsorption site is equivalent and the ability of a molecule to bind at an adsorption site is independent of whether the neighboring sites are occupied. This situation may be realistic when the surface coverage is low, but as many biomolecules are charged the central assumption of the Langmuir isotherm is unlikely to describe their adsorption over a wide range of surface coverage. Delahay and Mohilner⁶ have however considered the adsorption of a

neutral species at an electrode which obeyed the logarithmic Temkin isotherm where the driving force for adsorption (the free energy of adsorption) changes linearly with the number of filled binding sites and an approximation of half coverage is made.

$$b\Gamma = h(q) + RT \ln(a) \quad (1)$$

Γ is surface coverage, a is the solution activity of the adsorbing species, b is a constant, and $h(q)$ is a quantity that is a function of the charge density. The recent interest in the interaction of biomolecules with surfaces has resulted in a revival in attempts to describe kinetics of adsorption.⁷ Rahn and Hallock⁸ reported the kinetics of antibody binding to antigen-coated substrates followed by surface plasmon resonance. They fitted surface coverage data to an empirical exponential model:

$$\frac{\Gamma(t)}{\Gamma_f} = 1 - \exp(-kt^\alpha) \quad (2)$$

Equation 2 is based on a diffusion-limited model with adsorption proportional to the fraction of free sites, in which case $\alpha = 1/2$ (see below). Γ_f is an arbitrary value for the maximum coverage to allow for different configurations of adsorbed species at different solution concentrations. Data followed the theoretical $\alpha = 1/2$ at low concentrations but approached $\alpha = 1/4$ at higher concentrations of antibody. Peterlinz and Georgiadis⁹ also used surface plasmon resonance to study self-assembly by alkane thiols with increasing chain length. They concluded that in heptane there is one single, rapid kinetic step, while in ethanol there are at least three steps. The first step fits both a diffusion-limited model and a second-order Langmuir adsorption model. The second step is zero order, and overall the data imply a complex series of reactions.

- (1) Collings, A. F.; Caruso, F. *Rep. Prog. Phys.* **1997**, *60*, 1397.
- (2) Gooding, J. J.; Hibbert, D. B. *Trends Anal. Chem.* **1999**, *18*, 525.
- (3) Delahay, P.; Fike, C. J. *Am. Chem. Soc.* **1958**, *80*, 2628.
- (4) Delahay, P.; Trachtenberg, I. *J. Am. Chem. Soc.* **1957**, *79*, 2355.
- (5) Reinmuth, W. H. *J. Phys. Chem.* **1961**, *65*, 473.
- (6) Delahay, P.; Mohilner, D. M. *J. Am. Chem. Soc.* **1962**, *84*, 4247.

- (7) Peterlinz, K. A.; Georgiadis, R. M.; Herne, T. M.; Tarlov, M. J. *J. Am. Chem. Soc.* **1997**, *119*, 3401.
- (8) Rahn, J. R.; Hallock, R. B. *Langmuir* **1995**, *11*, 650.
- (9) Peterlinz, K. A.; Georgiadis, R. *Langmuir* **1996**, *12*, 4731.

The binding of ligands by receptors immobilized in a gel has been studied by Schuck and Minton.¹⁰ They consider the effect of mass transport on binding reactions of human interleukin to its receptor studied by a resonant mirror biosensor. The two-compartment model only treats transport from a bulk compartment to a surface compartment and thus is computationally easier to implement than a full simulation.

The adsorption of neutral molecules from solution is known to often show non-Langmuirian behavior.¹¹ The activity of an adsorbed species ($f(\Gamma)$) may be related to the standard free energy of adsorption (ΔG°):

$$f(\Gamma) = a \exp(-\Delta G^\circ/RT) = a\beta \quad (3)$$

a is a constant. Consideration of forces between adsorbed molecules leads to different isotherms. The most simple case is the Langmuir isotherm which has $f(\Gamma) = \text{constant}$, arising from an absence of intermolecular forces. Repulsion between molecules, which is determined by the parameter g , which is proportional to the coverage leads to

$$f(\Gamma) = a\beta_{\theta=0} \exp(-2g\Gamma/RT) \quad (4)$$

and the Frumkin isotherm (see theory section). If the energy of adsorption varies more quickly at low coverages, then the Freundlich approach, which has the energy of adsorption proportional to $\log(\Gamma)$, applies. The problem with the resulting isotherm is that it becomes singular at $\theta = 0$.

We have developed a number of biosensors in which enzymes are covalently bonded to carboxylic acid terminated alkane thiols.^{2,12–15} In fabricating these sensors, and particularly for sensors with more than one enzyme type,¹⁴ it is useful to understand the kinetics of the binding of an enzyme to the alkanethiolate self-assembled monolayer. In this paper, we discuss the validity of previously published kinetic models and compare the results of a full numerical simulation to the predictions from these different approximations. We will show that none of the approximate analytical models can describe the full range of our data but a numerical solution of a diffusion model with rate-limiting adsorption with heat of adsorption proportional to coverage does fit our data. Furthermore, we also fit the adsorption data modeled by Rahn and Hallock,⁸ and the data of Peterlinz et al.⁷ show that the full range of surface coverage can be described by the one simple model without necessitating assumptions of protein reconfiguration.

Theory

The relation between the rate of change of surface coverage and concentration (c) gradient at the surface is described by

$$\frac{\partial \Gamma}{\partial t} = D \left(\frac{\partial c}{\partial x} \right)_{x=0} \quad (5)$$

where D is the diffusion coefficient of the adsorbing species. The concentration gradient in turn may be determined by

- (10) Schuck, P.; Minton, A. P. *Anal. Biochem.* **1996**, *35*, 262.
 (11) Delahay, P. *Double layer and electrode kinetics*; Interscience Publishers: New York, 1965.
 (12) Gooding, J. J.; Hall, E. A. H.; Hibbert, D. B. *Electroanalysis* **1998**, *10*, 1130.
 (13) Gooding, J. J.; Situmorang, M.; Erokhin, P.; Hibbert, D. B. *Anal. Commun.* **1999**, *36*, 225.
 (14) Gooding, J. J.; Pugliano, L.; Hibbert, D. B.; Erokhin, P. *Electrochem. Commun.* **2000**, *2*, 217.
 (15) Gooding, J. J.; Erokhin, P.; Hibbert, D. B. *Biosens. Bioelectron.* **2000**, *15*, 229.

diffusion in the solution, kinetics at the surface, or both. Analytical solutions exist for several limiting systems discussed below.

Diffusion-Controlled Kinetics. With diffusion-controlled adsorption kinetics, the concentration of the adsorbing species adjacent to the surface will be significantly lower than the bulk concentration of this species. For semi-infinite plane diffusion to a surface for which the concentration at the surface ($x = 0$) is zero for all t ,

$$\left(\frac{\partial c}{\partial x} \right)_{x=0} = \frac{c_b}{\sqrt{\pi D t}} \quad (6)$$

where c_b is the bulk concentration. Equation 6 was derived by Ilkovic¹⁶ and is the basis of the Cottrell equation for the current at an electrode at which a reactant is completely consumed. The assumption of zero concentration at the surface is valid for the electrochemical case in which the adsorbing species is consumed at the electrode and therefore there is no end to the capacity for reaction. With a surface that can only support a monolayer, the assumption must eventually fail as surface sites are filled. Equations 5 and 6 give

$$\frac{\partial \Gamma}{\partial t} = \frac{D^{1/2} c_b}{\pi^{1/2} t^{1/2}} \quad (7)$$

and after integration with $\Gamma(t = 0) = 0$,

$$\Gamma = \frac{2D^{1/2} c_b}{\pi^{1/2}} t^{1/2} \quad (8)$$

Equation 8 predicts a continuous increase in Γ with time. In reality, the surface coverage cannot exceed some maximum value Γ_{\max} .

Rahn and Hallock⁸ extended the Ilkovic solution to allowed for a maximum surface coverage by considering the diffusion-limited case in which the rate is also proportional to the fraction of free surface ($1 - \theta$):

$$\frac{\partial \Gamma}{\partial t} = \frac{D^{1/2} c_b}{\pi^{1/2} t^{1/2}} (1 - \theta) \quad (9)$$

Integration of eq 9 gives

$$\frac{\Gamma}{\Gamma_{\max}} = \theta = 1 - \exp\left(-\left(\frac{t}{T}\right)^{1/2}\right) \quad (10)$$

where $T = \pi \Gamma_{\max}^2 / 4 D c_b^2$. An important aspect of eq 10 is that in theory all the parameters can be determined experimentally. Rahn and Hallock introduced the parameter Γ_{\max} , which is not Γ_{\max} , to allow for different configurations of adsorbate. The practical consequence of introducing Γ_{\max} is that T becomes a parameter to be fitted along with the exponent (α in eq 2). We note that k in eq 2 is $T^{-1/2}$ in eq 10 if $\alpha = 1/2$.

Delahay and Trachtenberg⁴ solved the diffusion equation for a linearized Langmuir isotherm. They write the Langmuir isotherm as

$$\frac{\Gamma}{\Gamma_{\max}} = \frac{c}{a + c} \quad (11)$$

for which the linear approximation is $\Gamma = K c_{x=0}$ where $K = \Gamma_{\max} / c_b$. Solution of eq 5 with this boundary condition

leads to the expression

$$\frac{\Gamma_t}{\Gamma_e} = 1 - \exp\left(\frac{D\theta}{K^2}\right) \operatorname{erfc}\left(\frac{D^{1/2}t^{1/2}}{K}\right) \quad (12)$$

where Γ_e is the equilibrium coverage and D is the diffusion coefficient. Delahay notes that eq 12 approaches equilibrium only very slowly.

Adsorption-Controlled Kinetics. At the other extreme, diffusion can be faster than the adsorption process, leading to kinetics that is determined by the rate of adsorption (and desorption if the process is reversible). A consequence of adsorption being kinetically controlled is that the concentration of the adsorbing species adjacent to the surface will approach the bulk concentration. Therefore, the rate of adsorption is first order in the adsorbing species and first order in the free sites at the surface (Langmuir-like behavior).

$$\frac{\partial \Gamma}{\partial t} = k_{\text{ads}} c_b (\Gamma_{\text{max}} - \Gamma) \quad (13)$$

Equation 13 may be integrated to give the coverage with time, assuming c_b and k_{ads} remain constant.

$$\Gamma = \Gamma_{\text{max}} (1 - \exp(-k_{\text{ads}} c_b t)) \quad (14)$$

We also consider two kinetic models with nonlinear dependence on coverage. First, the heat of adsorption is taken to be linearly dependent on coverage, that is, $\Delta H_{\text{ads}} = \Delta H_{\text{ads}}^0 (1 - \theta)$, which gives

$$k_{\text{ads}} = K_{\text{ads}}^0 \exp\left(\frac{\Delta H_{\text{ads}}}{RT}\right) = K_{\text{ads}} \exp(-b\theta) \quad (15)$$

where b is a constant ($= \Delta H_{\text{ads}}^0 / RT$) and $\theta = \Gamma / \Gamma_{\text{max}}$ and other constant terms have been incorporated into K_{ads} ($K_{\text{ads}} = K_{\text{ads}}^0 \exp(\Delta H_{\text{ads}}^0 / RT)$). Equation 13, when expressed in terms of the fractional coverage, becomes

$$\frac{\partial \theta}{\partial t} = k_{\text{ads}} c_b (1 - \theta) = K_{\text{ads}} c_b (1 - \theta) \exp(-b\theta) \quad (16)$$

For a reversible system, addition of the term for the rate of desorption to eq 16 leads to a Frumkin isotherm or, if the term $\theta / (1 - \theta)$ were set to 1 (i.e., when $\theta \approx 0.5$), the Temkin isotherm.^{17,18}

A logarithmic dependence of the heat of adsorption on θ , which is postulated in deriving the Freundlich isotherm, gives for $\theta > 0$

$$\frac{\partial \theta}{\partial t} = k_{\text{ads}} c_b (1 - \theta) = K_{\text{ads}} c_b (1 - \theta) \theta^{-b} \quad (17)$$

Unlike the Langmuir case in eq 14, there are no explicit solutions for the rate equations, eqs 16 and 17, but they can be solved numerically.

Numerical Solution of Adsorption with Diffusion. The failure of any one analytical solution to fully describe the reaction–diffusion system defined by the adsorption to a solid substrate over the range from adsorption to diffusion limited necessitates a numerical solution. The reaction–diffusion system can be described by Fick's second law ($dC/dt = D(d^2C/dx^2)$) with appropriate boundary conditions to define the surface adsorption process.

To employ a fully implicit solution of Fick's equations with adsorption at a surface at $x = 0$ as outlined by Britz¹⁹ requires writing Fick's second law in nondimensional terms. We define the following dimensionless variables: $C = c/c_b$, $T = t/\tau$ where τ is the experimental observation time, $X = x/\sqrt{D\tau}$, $K = c_b\sqrt{D\tau}/\Gamma_{\text{max}}$, $\theta = \Gamma/\Gamma_{\text{max}}$, $\alpha = D(\Delta t/\Delta x^2) = \Delta T/H^2$, where Δt and Δx are the time and distance steps, respectively, and ΔT and H are their dimensionless equivalents, and $G = dC/dX|_{x=0}$. The differential equation to solve becomes

$$\frac{dC}{dT} = \alpha \frac{d^2C}{dX^2} \quad (18)$$

The forward implicit method requires solution of the equation $\mathbf{A}C^+ = C$, where \mathbf{A} is the tridiagonal matrix with elements $-\alpha$, $1 + 2\alpha$, $-\alpha$, and C^+ is the vector of concentrations at $t = t + \Delta t$. The boundary condition for C at $x = 0$ is determined from the slope of the concentration which is $G = V_f/K$, where V_f is the adsorption rate in terms of whatever model is being adopted. Britz gives a method to smooth out the determination of the slope of the concentration at the boundary by taking the concentrations five cells out from the surface.

$$G_n = \frac{1}{a_n H} \sum_{i=0}^{n-1} b_{n,i} C_i \quad (19)$$

where $a_5 = 12$ and $b_{n,0-4} = -25, 48, -36, 16, -3$. The simulation was continued out to $X = \sqrt{6/H}$ at which point the boundary condition $C = 1$ was imposed. During the simulation, the value of C at the penultimate point was monitored and was always greater than 0.99.

The following expressions for the dimensionless rate of surface reaction were used.

$$V_f = k C_1 \tau (1 - \theta) \quad (\text{Langmuir}) \quad (20)$$

$$V_f = k C_1 \tau (1 - \theta) \exp(-b\theta) \quad (\text{Frumkin}) \quad (20a)$$

$$V_f = k C_1 \tau (1 - \theta) \theta^{-b} \quad (\text{Freundlich}) \quad (20b)$$

where C_1 is the concentration in solution at the first grid point (i.e., the one adjacent to the adsorbing surface) and the names relate to the corresponding isotherms. Equations 20, 20a, and 20b are nondimensional forms of eqs 14, 16, and 17, respectively.

The simulation proceeds as follows. For $T = 0$, $C = 1$ and $\theta = 0$ for all grid points. At time T , for given values of θ and C , V_f is calculated from eq 20. θ is updated by $V_f \Delta T$, and the forward difference matrix is solved for C^+ using the slope calculated from eq 19.

The algorithm was implemented in MatLab 5.3 (The MathWorks Inc., Natick, MA). For systems for which D , c_b , and Γ_{max} are known, only the adsorption rate constant k and the constant b defined in eqs 20a and 20b need to be fitted.

Experimental Section

Formation of Glucose Oxidase on Thiol Self-Assembled Monolayers. *Reagents.* Glucose oxidase (EC 1.1.3.4) from *Aspergillus niger* (type VII-S), 3-mercaptopropionic acid (MPA), 1-ethyl-3-(3-dimethylaminopropyl) carbodiimide hydrochloride (EDC), and *N*-hydroxysuccinimide (NHS) were obtained from Sigma Chemical Co. (Sydney, Australia). Reagent grade K_2HPO_4 ,

(17) Delahay, P. *Double layer and electrode kinetics*; Interscience Publishers: New York, 1965.

(18) Parsons, R. *J. Electroanal. Chem.* **1964**, 7, 136.

(19) Britz, D. *Digital Simulation in Electrochemistry*, 2nd ed.; Springer-Verlag: New York, 1988.

KH₂PO₄, and KCl were purchased from Ajax Chemicals Pty. Ltd. (Sydney, Australia). The pH of all buffer solutions was adjusted with either dilute NaOH or HNO₃. All reagents were used without further purification. Milli Q grade reagent water was used for all solutions.

QCM Measurement Protocol. The microbalance used was a home-built instrument based upon the circuitry described by Bruckenstein and Shay.²⁰ The quartz crystals were attached to a thermostated glass cell using a silicone rubber sealant so that only one face was in contact with the solvent. The temperature of the solution was controlled at 25.0 ± 0.1 °C with a Thermoline Unistat II heater/circulator to minimize frequency drift associated with thermal fluctuations. The typical stability of the balance when filled (10 mL) with a variety of solvents was ± 2 Hz over a period of about 1 h and ± 10 Hz over time scales of 5 h.

The gold surfaces of the crystals were cleaned with a "piranha" solution which comprises 1:3 (v/v) 30% H₂O₂/H₂SO₄, for 2 min. The crystals were then rinsed with copious amounts of ethanol followed by water prior to modification steps. (*Warning: piranha solution reacts violently with organic material and has been known to explode when stored in closed containers!*) Cleaned gold electrodes were modified by placing them into a 75:25 (v/v) ethanol/water solution containing 0.01 M MPA overnight. Modified electrodes were then washed in a 75:25 (v/v) ethanol/water solution and dried in a nitrogen stream. The MPA-modified electrodes were activated for 1 h in an aqueous solution at pH 5.5 containing 0.002 M EDC, 0.005 M NHS, 0.05 M phosphate, and 0.05 M KCl. Buffer (pH 5.5) was then introduced into the thermostated cell, and the output frequency of the crystal was monitored until a stable baseline was evident (typically 1 h). Before the addition of the protein solution, several small aliquots of buffer were injected into the cell as blank additions. An aliquot of the buffer solution containing the enzyme was then introduced into the cell. These solutions were maintained at the same temperature as the cell to avoid thermal disruptions from the injections, and the solutions were sufficiently concentrated to allow small injection volumes. All injections were accompanied by stirring for a 10 s period to ensure thorough mixing. Stirring was accomplished with a magnetic stirrer and a Teflon-coated stirrer bar. The typical initial buffer volume in the thermostated cell was 9.0 mL and injections were usually 200 μ L.

Results and Discussion

Stability and Efficiency of the Mathematical Method. The implicit method is stable and efficient, but it is necessary to ensure that the change in surface concentration ($V_f \Delta T$) does not perturb θ to the extent that the integration becomes unstable. In our experience, this was not a problem, but a fast adsorption could create a stiff system.

The two-compartment model¹⁰ would not be of great use here, as it requires steady-state conditions with the derivative of the concentration in the surface compartment to be much less than the derivative of the bulk concentration. This may hold at some times in the system here but would not pertain for all situations. Also, the power of present-day mathematical models allows exact solutions to be achieved on commonly available computers, obviating the need for semiempirical approximations.

Comparison between Models. To quantify the competition between adsorption and diffusion, we define the dimensionless parameter Φ :

$$\Phi = \frac{k_{\text{ads}} \tau \Gamma_{\text{max}}}{c_b \sqrt{D\tau}} \quad (21)$$

For $\Phi \ll 1$, the kinetics will be controlled by the rate of adsorption, while $\Phi \gg 1$ will lead to diffusion control.

For the kinetically controlled case with a linear isotherm (eq 20), the numerical simulation follows eq 14 as may be

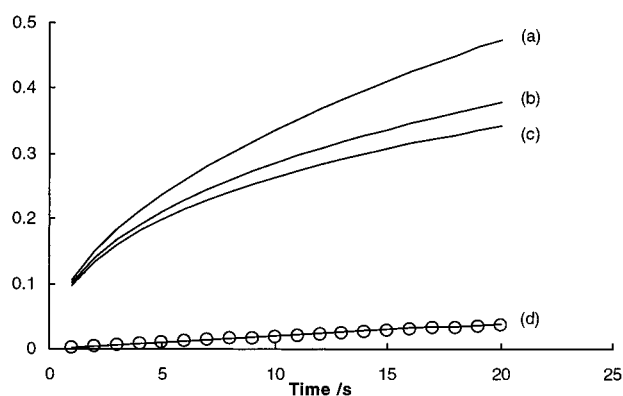


Figure 1. Adsorption for which the kinetics is limited by adsorption $\Phi = 0.095$ (see eq 21). Analytical models: (a) diffusion limited (Ilkovic equation, eq 6); (b) diffusion limited with rate proportional to free surface (eq 10), $\tau = 88.8$ s; (c) diffusion with Langmuir adsorption eq 12, $K = 7.52 \times 10^{-5}$ m; (d) adsorption limited eq 14, $k_{\text{ads}} = 15.0 \text{ s}^{-1} \text{ mol}^{-1} \text{ m}^3$. Circles are from the numerical solution of eq 5 with boundary surface kinetics from eq 20. $D = 5 \times 10^{-11} \text{ m}^2 \text{ s}^{-1}$, $\Gamma_{\text{max}} = 1 \times 10^{-12} \text{ mol cm}^{-2}$, $c_b = 1.33 \times 10^{-4} \text{ mol m}^{-3}$ ($= 20 \mu\text{g mL}^{-1}$ glucose oxidase).

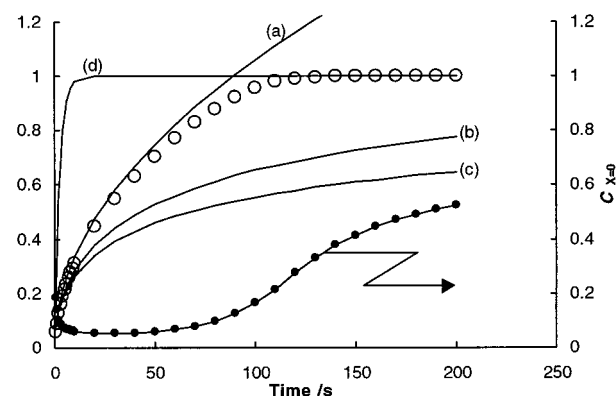


Figure 2. Adsorption for which the kinetics is limited by diffusion $\Phi = 60.2$ (see eq 21). Analytical models: (a) diffusion limited (Ilkovic equation, eq 6); (b) diffusion limited with rate proportional to free surface (eq 10), $\tau = 88.8$ s; (c) diffusion with Langmuir adsorption eq 12, $K = 7.52 \times 10^{-5}$ m; (d) adsorption limited eq 14, $k_{\text{ads}} = 3007 \text{ s}^{-1} \text{ mol}^{-1} \text{ m}^3$. Circles are from simulation (see Figure 1 for details). The line with filled circles (right-hand axis) is the concentration in the solution at the surface as a fraction of c_b .

expected (Figure 1) for an adsorption-limited process. Figure 1 also shows that, again as expected, the diffusion-limited theories predict a much faster rate of adsorption.

One of the assumptions of the solution which gives rise to eq 11 is that the concentration of the adsorbing species directly adjacent to the surface will approach the bulk concentration. Calculation, using the numerical simulation, shows that the concentration of adsorbing molecule in solution at the surface remains above $0.8c_b$ throughout the time period investigated, indicating only a small diffusion effect.

When the rate constant for adsorption is increased such that $\Phi = 60.2$, the rate-limiting step will be diffusion to the surface. Unlike the adsorption-limited case, none of the analytical theories predict the adsorption behavior of the more complete numerical simulation. The adsorption-limited theory, which neglects any mass transport effects, would result in the surface rapidly becoming saturated (curve d in Figure 2). Apart from small times and low surface coverage, neither the diffusion model of Rahn and Hallock with rate proportional to free surface (eq 10) nor diffusion with a linearized Langmuir isotherm solved by

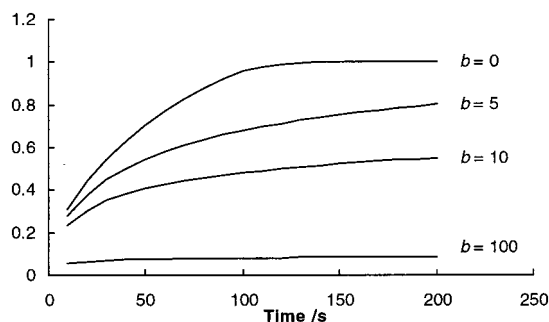


Figure 3. Numerical simulation of adsorption with kinetics proportional to the fraction of free sites and heat of adsorption proportional to the fraction of adsorbed sites (Frumkin). $D = 5 \times 10^{-11} \text{ m}^2 \text{ s}^{-1}$, $\Gamma_{\text{max}} = 1 \times 10^{-12} \text{ mol cm}^{-2}$, $c_0 = 1.33 \times 10^{-4} \text{ mol m}^{-3}$ ($= 20 \mu\text{g mL}^{-1}$ glucose oxidase), $k = 0.4 \text{ s}^{-1}$. Values of b on curves for the rate of adsorption are given by $k a_0(1 - \theta) \exp(-b\theta)$.

Delahay and Trachtenberg (eq 12) fully describes the nonlimiting simulated data. The simulated rate does however follow the Ilkovic equation reasonably well until the surface is about 80% filled. At this point, the effect of the $(1 - \theta)$ term in eq 20 causes the coverage to go asymptotically to unity while the Ilkovic equation continues to allow surface adsorption due to the failure of this model to allow for filling of surface sites. Also shown in Figure 2 is the concentration of the adsorbate next to the surface (c_0), as predicted from the numerical simulation (see right-hand axis). At low surface coverage, c_0 approaches zero and hence the assumption of the diffusion-limited models of $c_0 = 0$ holds. As the surface begins to fill, however, the concentration of the adsorbate next to the surface begins to rise at about the same point where the Ilkovic equation begins to fail. Hence, the condition of diffusion limitation is no longer valid and the kinetics of adsorption is beginning to be limited by the adsorption step.

It is clear from the discussion of the comparison between the numerical model and the various analytical solutions published that none of the analytical solutions can fully describe the adsorption kinetics over a wide range of experimental conditions.

Nonlinear Adsorption Kinetics. The analytical models and the numerical simulation used in Figures 1 and 2 all assume Langmuirian type adsorption. The independence of adsorption sites assumed by Langmuir adsorption would be expected to hold at low surface coverage, but as surface sites become filled, in the case of charged biomolecules, the adsorption kinetics is expected to deviate from linearity. The effect of nonlinear adsorption kinetics can easily be investigated via altering the surface kinetic boundary conditions in the numerical simulation. Introducing nonlinear adsorption kinetics has the result of lowering the rate of adsorption. The Frumkin-like equation (eq 20a) leads to a range of curves that may be tuned by varying the parameter b (Figure 3). When there is no change in heat of adsorption with coverage (which is equivalent to setting $b = 0$), the Frumkin isotherm reduces to the Langmuir case. The numerical simulation predicts significant deviations from the Langmuir type behavior for values of b that correspond to typical heats of adsorption even if the fraction of filled sites (θ) is small.

Turning attention to Freundlich type behavior (eq 20b), it proved difficult to simulate using the model with θ^{-b} because of the magnitude of the term at values of θ near zero. The simulations of Figure 4 were started at $\theta = 0.1$. Fitting experimental data to eq 20b also proved difficult. The rates of the reaction that we have studied and those

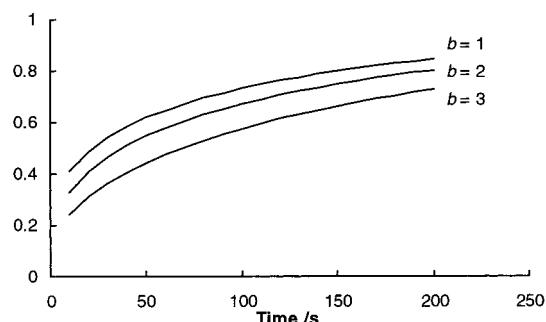


Figure 4. Numerical simulation of adsorption with kinetics for which the heat of adsorption is proportional to the fraction of adsorbed sites raised to a power (Freundlich). $D = 5 \times 10^{-11} \text{ m}^2 \text{ s}^{-1}$, $\Gamma_{\text{max}} = 1 \times 10^{-12} \text{ mol cm}^{-2}$, $c_0 = 1.33 \times 10^{-4} \text{ mol m}^{-3}$ ($= 20 \mu\text{g mL}^{-1}$ glucose oxidase), $k = 0.004 \text{ s}^{-1}$. Values of b on curves for the rate of adsorption are given by $k a_0(1 - \theta)\theta^{-b}$.

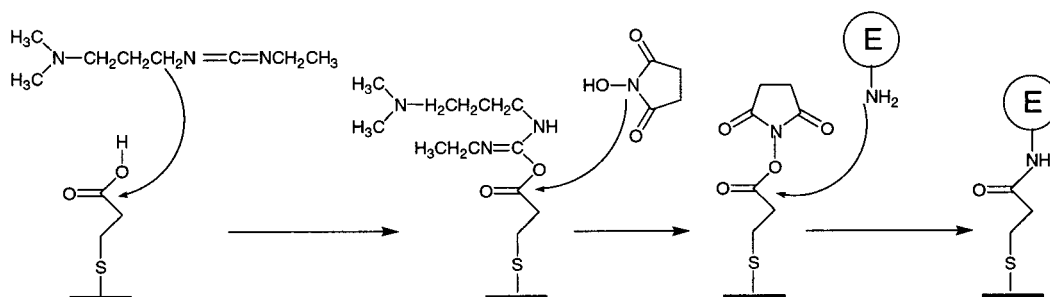
of other studies all imply that there is some factor that slows the reaction as it proceeds over and above the effect of filling the available sites. All the nonlinear approaches provide models for the decrease in magnitude of the heat of adsorption as coverage increases, but only the Frumkin model has the correct form to cover concentration and time ranges that lead to either very low coverage or coverage that reaches Γ_{max} .

Fitting Data for the Reaction of Glucose Oxidase at a Self-Assembled Monolayer. To demonstrate the utility of the numerical model over the limiting analytical solutions, the kinetics of the adsorption of glucose oxidase (GOD) onto a MPA self-assembled monolayer (SAM) was monitored using a quartz crystal microbalance. The MPA surface was activated to allow covalent attachment of the enzyme by converting the terminal carboxylic acid moiety to a succinimidyl ester which was then susceptible to nucleophilic attack from amine groups on free lysine groups on the enzyme surface (see Scheme 1). Hence, the adsorption reaction is irreversible and not particularly fast.

Variation of the concentration of glucose oxidase in solution provides a useful system to observe kinetics that is limited by the reaction at low solution concentrations and diffusion for greater solution concentrations. We have measured the maximum monolayer coverage of GOD as $1 \times 10^{-12} \text{ mol cm}^{-2}$ ¹³ and take the diffusion coefficient as $5 \times 10^{-7} \text{ cm}^2 \text{ s}^{-1}$ for a 10 nm diameter particle.²¹ With these figures, none of the approximate diffusion equations predict θ values other than 1; that is, the observed reaction is much slower than it would be if it were diffusion controlled. This also can be seen in the disparity of time axes between the simulated plots of Figures 1–4 and the experimental data of Figure 5. A slow adsorption has been reported for antibody–antigen reactions by Rahn and Hallock⁸ who rationalize the kinetics in terms of orientation requirements and the exclusion of free surface by large adsorbed molecules. To attempt to fit these data to existing models requires unrealistically small values of D or Γ_{max} .

We have been able to fit a wide range of data using our numerical simulation and a Frumkin-like rate equation (eq 20a). Figure 5 shows fitted data with $k_{\text{ads}} = 18\,000$ ($\sigma = 12\,000$) $\text{M}^{-1} \text{ s}^{-1}$ and $b = 7.5$ ($\sigma = 4.4$) (eq 20a) for the experimental range of solution concentrations of GOD. In the fit using eq 20a, although there are reasonably high standard deviations on the values for k and b , there is no trend with c_0 . Inspection of the concentration values at

(21) Weast, R. E. *Handbook of Chemistry and Physics*, 53rd ed.; CRC Press: Cleveland, 1972.

Scheme 1 Reaction Sequence for the Preparation of the Enzyme-Modified Gold Surfaces^a

^a The adsorption kinetics monitored using the quartz crystal microbalance for the data shown in Figure 5 relate to the final step, the covalent attachment of GOD to the activated SAM surface.

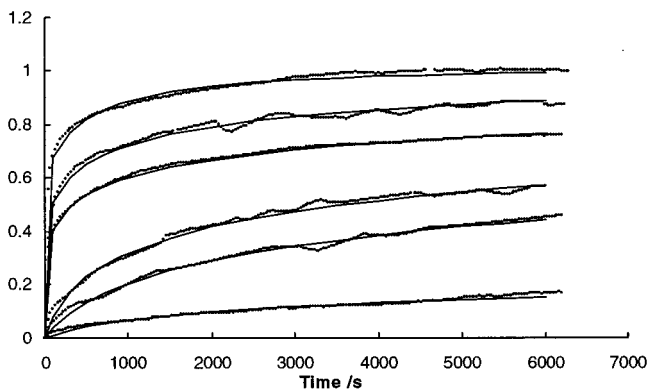


Figure 5. Reaction of GOD at a self-assembled monolayer from solutions containing 480, 240, 120, 20, 8, and 1.6 $\mu\text{g mL}^{-1}$ GOD (upper curve to lower curve). Points are experimental data; solid lines are fit to a Frumkin isotherm with diffusion. $D = 5 \times 10^{-11} \text{ m}^2 \text{ s}^{-1}$, $\Gamma_{\text{max}} = 1 \times 10^{-12} \text{ mol cm}^{-2}$, and values of K_{ads} and b (eq 20a) are given in Table 1.

Table 1. Parameters of Fitted QCM Data for the Adsorption of GOD at a Thiolated Gold Surface with Rate Proportional to the Fraction of Free Sites and Heat of Adsorption Proportional to the Fraction of Adsorbed Sites (Frumkin)^a

[GOD] ($\mu\text{g mL}^{-1}$)	K (s^{-1})	K/α_b ($\text{M}^{-1} \text{ s}^{-1}$)	b
480	0.0589	18400	4.88
240	0.0407	25400	6.55
120	0.0301	37600	8.07
20	0.00104	7790	5.12
8	0.000425	7970	5.09
1.6	0.000128	12000	15.4

^a $D = 5 \times 10^{-11} \text{ m}^2 \text{ s}^{-1}$; $\Gamma_{\text{max}} = 1 \times 10^{-12} \text{ mol cm}^{-2}$. K and b are defined in eq 20a.

the surface reveals that the kinetics is limited by adsorption. The lowest solution concentration at the surface is $0.76\alpha_b$ found after 1200 s of reaction from the lowest concentration solution ($1.6 \mu\text{g mL}^{-1}$). An adsorption model following Freundlich kinetics does not fit the data well at low coverage and the fit is also poor if the linear (Langmuir) model is employed. In the latter case, approximate fits can only be achieved by allowing the diffusion coefficient to vary and become very small ($\sim 10^{-14} \text{ cm}^2 \text{ s}^{-1}$). The diffusion coefficient then becomes dependent on solution concentration.

The fact that the data presented here do not fit a Langmuir isotherm, and neither do those of many other protein systems, should not be a surprise as many biomolecules, including GOD, have net negative charges at the pH used and therefore adsorption of one biomolecule would be expected to inhibit the adsorption of the next purely using an electrostatic argument. The intermolecular repulsion would thus scale as the coverage and

lead to the observed isotherm and kinetics. However, even our kinetic model is likely to be a gross simplification. Atomic force microscopy imaging of glucose oxidase adsorbed onto self-assembled monolayers of alkanethiols shows the complex nature of the interactions when enzyme molecules associate into ordered clusters onto the surface after adsorbing onto the surface.²² In a 1998 review, Tengvall et al. writes, "The model experiments ... reveal that the detailed microscopic chemistry of the surface modification plays an important role for the biological response at short times".²³ In the case of glucose oxidase adsorbing onto a SAM surface, the adsorption sites are reasonably ill defined.

Fitting of Adsorption Data from the Literature for Surfaces with Well-Defined Adsorption Sites. In the case of glucose oxidase adsorbing onto a SAM surface, the adsorption sites are reasonably ill defined. In contrast, the antigen–antibody reactions investigated by Rahn and Hallock⁸ and oligonucleotide hybridization by Peterlinz and Georgiadis⁹ have recognition surfaces with well-defined binding sites (assuming adsorption occurs directly at the binding partner). As discussed above, Rahn and Hallock have monitored the adsorption of the antibody onto the antigen-modified surface (single site immunometric assays) using surface plasmon resonance. The adsorption data were fitted to a diffusion-controlled analytical model where the rate was proportional to the amount of free surface (eq 10). Equation 10 however only fitted the data at low concentrations of antigen in solution, while at high concentrations the adsorption data could be fitted if the power to which the exponential term in eq 10 was raised (α) was changed to $1/4$. The rationale for the decrease in α was a change in the shape of the adsorbing molecule from ellipsoidal to disklike as concentration increased. There is no direct evidence for such a molecular reconfiguration in solution. The Rahn and Hallock⁸ model however does start with the premise of Langmuirian type adsorption. Based on the same electrostatic argument employed for glucose oxidase above, the adsorption of one negatively charged antibody onto a surface could be expected to influence the energetics of subsequent antibody adsorption. Hence, we have fitted the Rahn and Hallock data, obtained from measurements of figures in their paper, to our numerical model using the Frumkin type adsorption isotherm employed for glucose oxidase (Figure 6).

The fits shown in Figure 6 were obtained with $k_{\text{ads}} = 570 \text{ M}^{-1} \text{ s}^{-1}$ and $b = 24.1$ when the concentration of rabbit antiovine serum albumin (RABSA) antibody in solution was $76.1 \mu\text{g/mL}$ and $k_{\text{ads}} = 1062 \text{ M}^{-1} \text{ s}^{-1}$ and $b = 5.53$

(22) Losic, D.; Gooding, J. J.; Shapter, J. G.; Hibbert, D. B.; Short, K. *Electroanalysis* **2001**, *13*, 1385.

(23) Tengvall, P.; Lundström, I.; Liedberg, B. *Biomaterials* **1998**, *19*, 407.

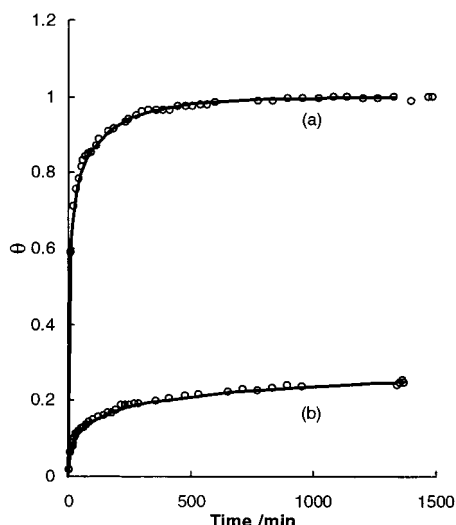


Figure 6. Adsorption of RABSA to a bovine serum albumin modified surface for solutions containing (a) 76.1 $\mu\text{g/mL}$ and (b) 2200 $\mu\text{g/mL}$ RABSA. Points are surface plasmon resonance data from Rahn and Hallock (ref 5), and solid lines are fits to a Frumkin isotherm with diffusion. For (a), $D = 5 \times 10^{-11} \text{ m}^2 \text{ s}^{-1}$, $\Gamma_{\text{max}} = 2.15 \times 10^{-8} \text{ mol m}^{-2}$, $k_{\text{ads}} = 570 \text{ M}^{-1} \text{ s}^{-1}$, and $b = 24.1$ (eq 20a), and for (b), $D = 5 \times 10^{-11} \text{ m}^2 \text{ s}^{-1}$, $\Gamma_{\text{max}} = 8.56 \times 10^{-8} \text{ mol m}^{-2}$, $k_{\text{ads}} = 1062 \text{ M}^{-1} \text{ s}^{-1}$, and $b = 5.53$.

when the concentration of RABSA antibody in solution was 2200 $\mu\text{g/mL}$ (eq 20a). The χ^2 values for each fit were 1.3×10^{-5} and 3.8×10^{-5} , respectively.

The adsorption of ss-DNA to a surface modified with complementary ss-DNA provides another system where a charged species adsorbs onto an interface as observed with the enzyme and antibody examples discussed above. Therefore, the Frumkin type isotherm coupled with diffusion should also fit DNA adsorption-time data for a

DNA recognition surface. Peterlinz et al. (see footnotes 3 and 4) have monitored DNA hybridization using surface plasmon resonance and fitted the isotherm to a diffusion-limited Langmuirian isotherm. These same data gave an excellent fit to the Frumkin type isotherm coupled with diffusion (data not shown) with $k_{\text{ads}} = 8980 \text{ M}^{-1} \text{ s}^{-1}$, $b = 2.8$, and $\chi^2 = 4.7 \times 10^{-4}$. Whether the hybridization of DNA at a surface conforms to a Langmuir or Frumkin isotherm cannot be determined from data from a single concentration of adsorbing ss-DNA in solution used here. We are currently monitoring DNA adsorption data using a quartz crystal microbalance to shed further light on this question.

It may be of interest to show that a diffusion-limited system is correctly fitted by the models discussed here by performing experiments in solutions with added glycerol and at lower temperatures. The increase in diffusion coefficient should be followed by the model.

Conclusions

We have demonstrated that limiting models based on Langmuirian adsorption for the kinetics of diffusion with irreversible adsorption fit neither numerical simulations nor experimental data for reaction of GOD at an alkane-thiolate self-assembled monolayer over a wide range of experimental conditions. Agreement between experiment and numerical simulation is achieved by a model that couples diffusion and irreversible adsorption in which the rate of surface reaction is proportional to the fraction of free sites and the magnitude of the heat of adsorption decreases linearly with coverage. This same adsorption model is shown to also describe the adsorption of an antibody to an antigen-modified surface and for the hybridization of DNA where one-half of the duplex is in solution and the other is attached to a surface.

LA015567N